New Journal of Physics
The open access journal at the forefront of physics

Deutsche Physikalische Gesellschaft DPG
IOP Institute of Physics

Published in partnership with: Deutsche Physikalische Gesellschaft and the Institute of Physics

OPEN ACCESS

RECEIVED
26 November 2019

REVISED
16 January 2020

ACCEPTED FOR PUBLICATION
3 February 2020

PUBLISHED
3 March 2020

PAPER

High-frequency spin transfer nano-oscillator based on the motion of skyrmions in an annular groove

Chendong Jin[1], **Yunxu Ma**[1], **Chengkun Song**[1], **Haiyan Xia**[1], **Jianing Wang**[1], **Chunlei Zhang**[1], **Zhaozhuo Zeng**[1], **Jianbo Wang**[1,2] and **Qingfang Liu**[1]

[1] Key Laboratory for Magnetism and Magnetic Materials of the Ministry of Education, Lanzhou University, Lanzhou 730000, People's Republic of China
[2] Key Laboratory for Special Function Materials and Structural Design of the Ministry of the Education, Lanzhou University, Lanzhou 730000, People's Republic of China

E-mail: liuqf@lzu.edu.cn

Keywords: spin transfer nano-oscillator, skyrmion, annular groove

Abstract

Magnetic skyrmion-based spin transfer nano-oscillators (STNOs) have been proposed as microwave signal generators and attracted enormous interest recently. However, the oscillation frequency of skyrmion-based STNOs is about 2 GHz, which is not so high for practical applications. In this paper, we create an annular groove in the surface of the free layer and put skyrmions in the annular groove. Due to the potential of the groove, skyrmions are confined to moving in the groove when driven by the spin-polarized currents. Through micromagnetic simulations, it is found that the frequency tunability of the STNO with the presence of the annular groove reaches to 15.63 GHz, which is more than 6 times higher than the case without the presence of the annular groove because of three reasons: the oscillation radius of skyrmions can be adjusted by the groove, the potential of the groove is larger than that of the edge and the groove can limit the diameter of skyrmions so that a larger number of skyrmions can be placed in the groove. Our results present the understanding of dynamic of skyrmions in an annular groove, which provides alternative possibilities for the design of skyrmion-based STNOs.

1. Introduction

Spin transfer nano-oscillators [1] (STNOs) are used to produce microwave signals, which have attracted large interest in recent years due to their outstanding advantages, such as the broad range of frequency, the lower working voltage, the small sizes and the wider working temperature. A simple structure of a STNO usually consists of two magnetic layers (a relatively thick fixed layer and a relatively thin free layer) that separated by a spacer layer. A DC current is polarized by flowing through the fixed layer which drives a steady precession of magnetization in the free layer. This precession can be detected as a microwave signal by either the giant magnetoresistance or the tunneling magnetoresistance effects. To date, STNOs are divided into various types according to the different configurations of free magnetic layers, such as a single domain [2, 3], magnetic vortices [4–6], magnetic droplets [7, 8] and magnetic skyrmions [9–14]. Different from these three-layered STNOs, there is an alternative single-layered magnetic oscillator that works based on the periodical motion (rotation [15–17] or translation [18]) of magnetic domain wall driven by spin currents or magnetic fields.

Magnetic skyrmions [19] are topologically protected chiral spin configurations. So far, different types of skyrmions including Bloch skyrmions, Néel skyrmions and Antiskyrmions have been observed in bulk lattices with *B*20 structure [20–22], heterostructures lacking interfacial inversion symmetry [23–25] and Heusler compounds [26] due to the presence of bulk Dzyaloshinskii–Moriya interaction [27] (DMI), interfacial DMI [28, 29] and anisotropic DMI [30], respectively. Moreover, because of the translational symmetry breaking on the surface of bulk chiral material, Twisted skyrmions are observed in Cu_2OSeO_3 below a critical thickness [31]. Recently, it is demonstrated that magnetic skyrmions can be excited into oscillation in a nanodisk by the

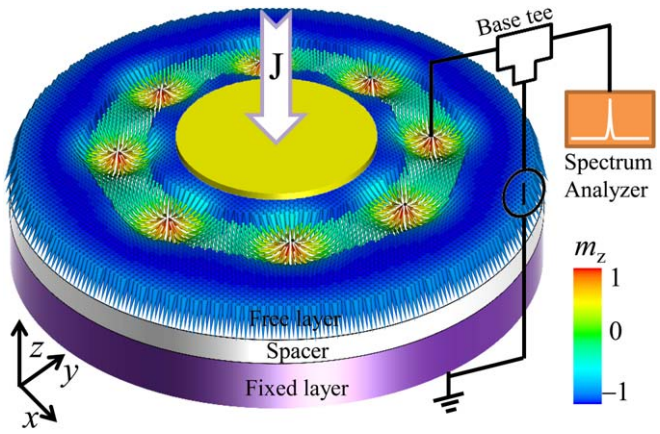

Figure 1. Schematic diagram of the STNO with an annular groove in the free layer. The color code indicates the out-of-plane component of the cones in the free layer: from blue, over green, to red represent where m_z is −1, 0 and 1, respectively. The white represents the spacer, and the purple indicates that the polarization vector of the fixed layer is along the $-z$ direction.

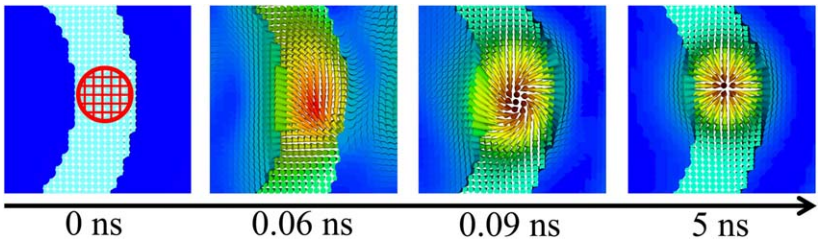

Figure 2. Creation of a skyrmion in the annular groove by injection of a 0.1 ns spin-polarized pulse. The injection region is marked by a red circle with the diameter of 10 nm, the current density is -100×10^{11} A m^{-2} with the polarization vector of the fixed layer along the $-z$ direction.

spin-polarized currents, which provides a possibility of skyrmion-based STNOs [9–11]. However, except that the oscillation frequency of antiferromagnetic skyrmion-based STNOs [12] can reach ten of GHz, ferromagnetic skyrmion-based STNOs only produce about 2GHz, which need a further improvement for applications. In this paper, we propose adding an annular groove to the free layer of ferromagnetic skyrmion-based STNOs. Then we investigate performance and oscillation frequency of the STNOs by using micromagnetic simulations. At last, we discuss the reasons for the increase in frequency of this type of STNOs by analyzing the Thiele's equation.

2. Model and simulation details

The skyrmion-based STNO is a sandwich structure, i.e, consisting a fixed layer, a spacer and a free layer, as shown in figure 1. The diameter of the nanodisk is 100 nm, and the thickness of the free layer is 1 nm with the mesh size of $1 \times 1 \times 0.5$ nm^3. We first create an annular groove with a depth of 0.5 nm in the free layer, and then set a single or multiple Néel skyrmions in the annular groove region. However, In addition to [32], which reported current-induced skyrmion motion guided by a groove. It is a challenge to create a groove experimentally. Here, we provide an idea for possible implementation of the groove: Néel skyrmions can be replaced by Bloch skyrmions, and therefore the thickness of the free layer, i.e. the cubic *B*20 chiral magnets can be slightly increased, which reduces the difficulty of digging the groove and possibly carried out by electron-beam lithography [33]. The creation of skyrmions can be achieved by a local perpendicular current injection, as shown in figure 2. A perpendicular spin-polarized current is injected into the annular groove at 0 ns. Under a continuous injection of current, skyrmion-liked structures are appeared as shown in the snapshots at 0.06 and 0.09 ns. The current is turned off at 0.1 ns and after a 4.9 ns long relaxation, a stable skyrmion is nucleated in the annular groove. The threshold current can be further reduced with the presence of a perpendicular magnetic field [34]. Therefore, a local perpendicular current injection combined with an external magnetic field may be easier to create the skyrmions in the annular groove experimentally. The skyrmions are confined in the annular groove due to the potential of the groove. With a continuous current vertically injecting into the sandwich

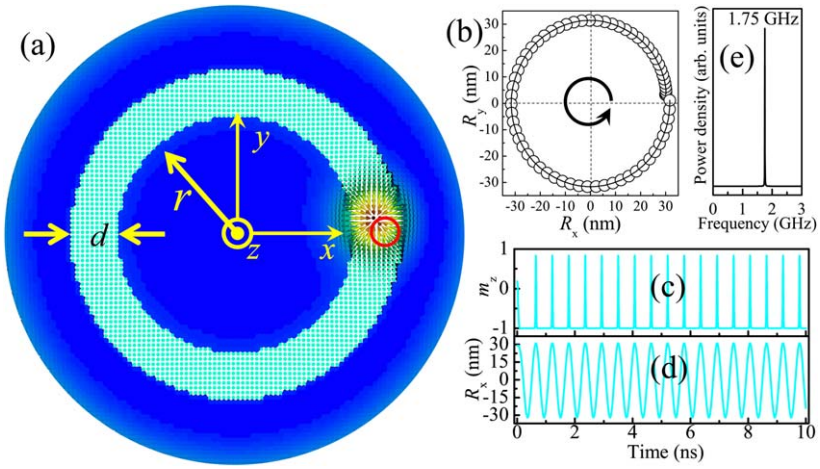

Figure 3. (a) Ground state of a single skyrmion-based STNO. d and r are fixed at 10 and 25 nm, respectively. The red circle region represents the detection area, whose diameter is 6 nm and coordinate of the center is (31.5, 0 nm). (b) The trajectory of the skyrmion in the nanodisk with the current density of 10×10^{11} A m^{-2}. (c) and (d) show the m_z in the detected region and R_x as a function of time, respectively. It should be noted that the total calculation time is 100 ns with the step of 0.01 ns, here only shows the first 10 ns. (e) FFT power spectrum of the STNO.

structure by a point contact electrode, the skyrmions begin to move around in the annular groove, and then a stable oscillation voltage signal can be detected when the skyrmions pass the region of detecting contact.

The micromagnetic simulation results are performed by using the Object Oriented MicroMagnetic Framework (OOMMF) public code [35] with the additional module for DMI. The Landau–Lifshitz–Gilbert (LLG) equation extended with the Slonczewski torque [36] is numerically solved for the dynamics of time-dependent magnetization, as follow:

$$\frac{\mathrm{d}\mathbf{m}}{\mathrm{d}t} = -\gamma \mathbf{m} \times \mathbf{H}_{\mathrm{eff}} + \alpha \mathbf{m} \times \frac{\mathrm{d}\mathbf{m}}{\mathrm{d}t} + \frac{u}{t_{\mathrm{F}}} \mathbf{m} \times (\mathbf{m}_{\mathrm{p}} \times \mathbf{m}), \tag{1}$$

where γ is the gyromagnetic ratio, $\mathbf{m}$ is the unit vector of the local magnetization, the Gilbert damping α is set to 0.5 and 0.02 for solving the ground state and the dynamic response procedure, respectively. t_{F} is the thickness of the free magnetic layer, $\mathbf{m}_{\mathrm{p}}$ is the polarization direction of the fixed layer along the $-z$ direction. u represents the spin-polarized electrons velocity with the form $u = \frac{\gamma \hbar P}{2\mu_0 e M_{\mathrm{s}}} J$, where J is the current density, e is the electron charge, P is the spin polarization, $\hbar$ is the reduced Planck constant, μ_0 is the permeability of free space, and M_{s} is the saturation magnetization. $\mathbf{H}_{\mathrm{eff}}$ is the effective field including the exchange field, perpendicular anisotropy field, demagnetization field and interfacial DMI effective field. The Oersted field induced by the current is neglected because of its little influence on the STNO [11]. The free layer is considered as a Co magnetic film on a heavy-metal substrate inducing the interfacial DMI. The material parameters of the free layer are from [11, 34, 37]: saturation magnetization $M_{\mathrm{s}} = 580 \times 10^3$ A m^{-1}, exchange constant $A = 1.5 \times 10^{-11}$ J m^{-1}, perpendicular magnetic anisotropy constant $K_{\mathrm{u}} = 8 \times 10^5$ J m^{-3}, DMI strength $D = 3.5 \times 10^{-3}$ J m^{-2}. These parameters guarantee the existence of Néel skyrmions in the nanodisk.

3. Results and discussion

3.1. A single skyrmion-based STNO

First we investigate the dynamics of a single skyrmion in the annular groove, as shown in figure 3. Figure 3(a) shows that the initial position of a skyrmion is located in the annular groove, where the width and inner radius of the annular groove are defined as d and r with the value of 10 and 25 nm, respectively. The radius of the point contact electrode is set to be equal to r, when the nanodisk is continuously injected current with the density of 10×10^{11} A m^{-2}, the skyrmion begin to move counterclockwise in the annular groove as shown in figure 3(b), which displays the guiding center (R_{x}, R_{y}) of the skyrmion in the Cartesian coordinate system. The form of the guiding center is given by [38]:

$$R_{\mathrm{x}} = \frac{\int\int xq\mathrm{d}x\mathrm{d}y}{\int\int q\mathrm{d}x\mathrm{d}y}, \; R_{\mathrm{y}} = \frac{\int\int yq\mathrm{d}x\mathrm{d}y}{\int\int q\mathrm{d}x\mathrm{d}y}, \tag{2}$$

where q is the topological density. One can see that the initial oscillation radius of the skyrmion is 30 nm, i.e. the initial position of the skyrmion is in the center of the groove. After applying a spin current, the oscillation radius

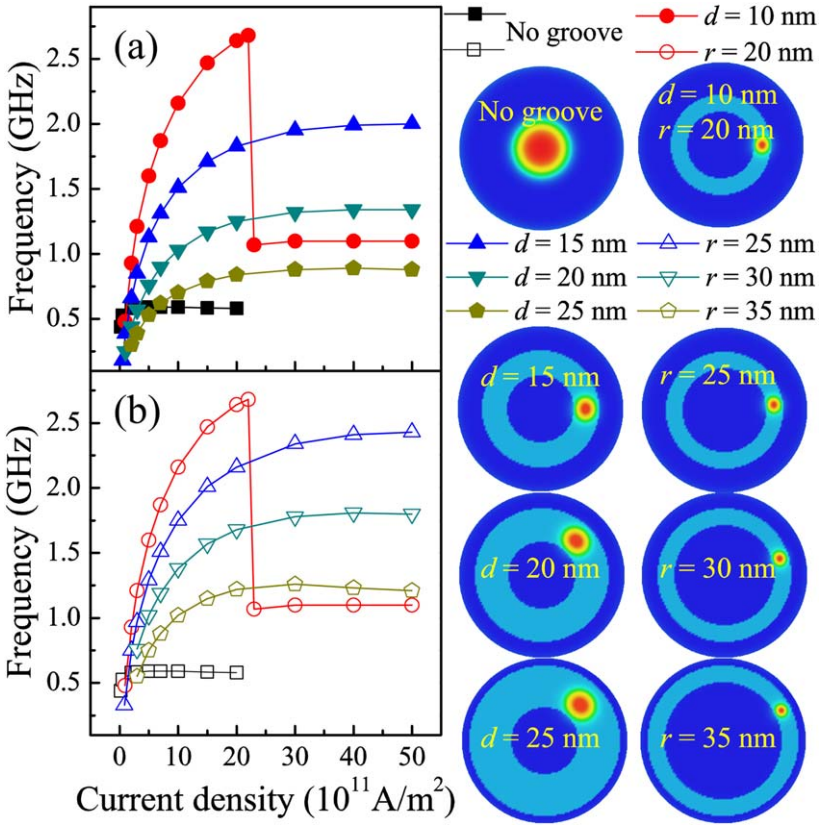

Figure 4. (a) Oscillation frequency as a function of current density for $d = 10$, 15, 20 and 25 nm with r fixed at 20 nm. (b) Oscillation frequency as a function of current density for $r = 20$, 25, 30 and 35 nm with d fixed at 10 nm. Snapshots in the right side show the ground state of a single skyrmion located in an annular groove with different d and r.

of the skyrmion increases to 31.5 nm, this means that there is a force from the outer kerb of the groove pushing the skyrmion back to the center of the groove. Figures 3(c) and (d) show the oscillations of the m_z in the detected region (the red circle region marked in figure 3(a)) and R_x, respectively. It can be seen that $m_z = 0.83$ indicates the skyrmion moving pass the detection area, and the time dependence of m_z is similar to that of R_x. The corresponding power spectrum shows that the frequency of a single skyrmion-based STNO is 1.75 GHz, which is obtained by taking fast Fourier transform of the oscillation of R_x, as shown in figure 3(e).

The different width and inner radius of the annular groove have an influence on the kerb force acting on the skyrmion and the oscillation radius of the skyrmion. Therefore, we then investigate the influence of d and r on the oscillation frequency of the STNO, as shown in figure 4. Figure 4(a) shows the oscillation frequency dependence of current density for different d with r fixed at 20 nm. For the case without the annular groove, the STNO starts to oscillate with the frequency of 440 MHz when current is applied with the density of 0.2×10^{11} A m^{-2}, with the current density further increases to 20×10^{11} A m^{-2}, the frequency of the STNO gradually increases to 590 MHz and then remains unchanged. For the case with the annular groove, the oscillation frequency is much larger than the case without the annular groove and decreases with the increase in d from 15 to 25 nm under the same current density. To be noted, for $d = 10$ nm, the frequency of the STNO drops from 2.68 to 1.1 GHz when the current density increases from 22×10^{11} A m^{-2} to 23×10^{11} A m^{-2}, this is because the gyrotropic force of the skyrmion exceeds the critical kerb force of the annular groove so that the skyrmion moves out of the annular groove. Figure 4(b) shows the frequency of the STNO versus the current density for different r with d fixed at 10 nm. It is found that the frequency of the STNO decreases with the increase in r from 25 to 35 nm under the same current density. The snapshot of the initial states of the STNO under different d and r are shown in the right side of figure 4. The presence of the annular groove not only increases the frequency of the STNOs but also limits the size of the skyrmion. Therefore, in the following simulations, in order to place more skyrmions in the annular groove and ensure that skyrmions do not move out of the annular groove, d and r are fixed at 10 and 25 nm, respectively.

3.2. Multiple skyrmions-based STNO

For the situation without the presence of the annular groove, there are at most 6 skyrmions with a centrosymmetric distribution that can stably exist in a single nanodisk, as reported in our previous work [9].

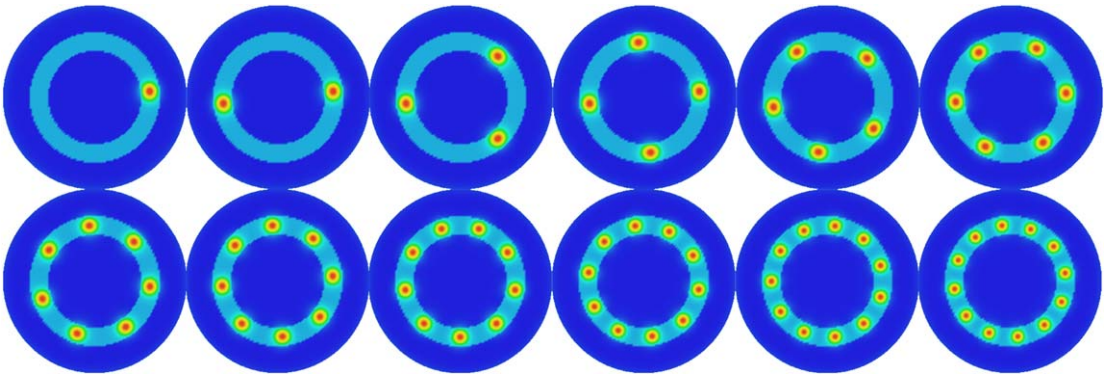

Figure 5. Snapshots of the ground states of STNO with 1–12 numbers of skyrmions in an annular groove.

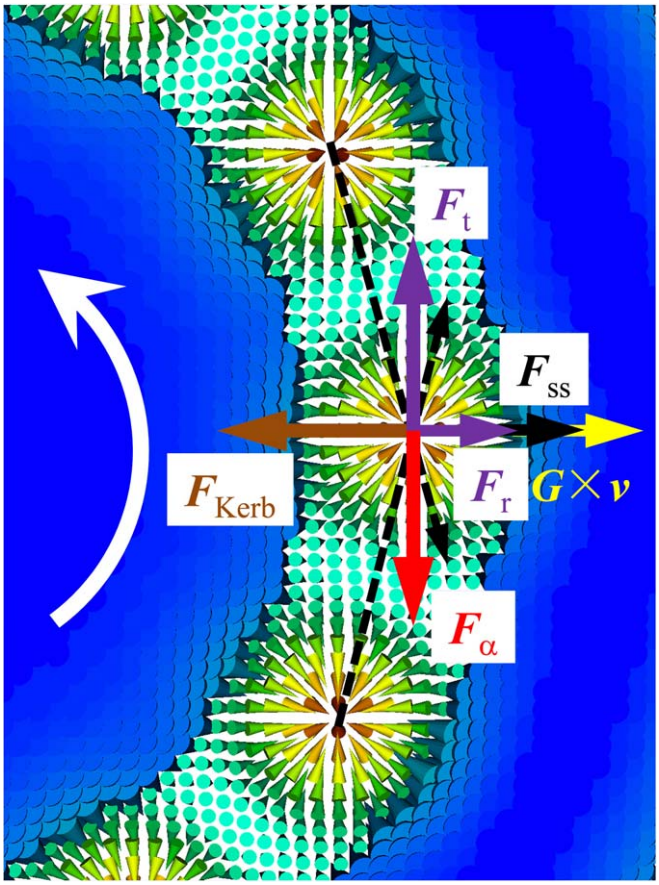

Figure 6. Schematic of the different forces affecting on one skyrmion in the annular groove. White arrow represents the move direction of skyrmions driven by a spin current.

When the number of skyrmions (N) is larger than 6, the skyrmions are pushed to the middle of the nanodisk or even annihilation due to the large repulsive force between the skyrmions. For the situation with the presence of the annular groove, because the size of the skyrmions are limited by the potential of the groove, the maximum number of skyrmions with a centrosymmetric distribution increases to 12, as shown in figure 5. The excitation of multiple skyrmions in the annular groove can be achieved by repeating the process of the excitation of a single skyrmion, as shown in figure 2. When the nanodisk is continuously applied a point contact spin current, all the skyrmions in the groove move with the counterclockwise mode.

The dynamic of one of multiple skyrmions in the annular groove as shown in figure 6 can be described by the Thiele's equation as follow [9, 39]:

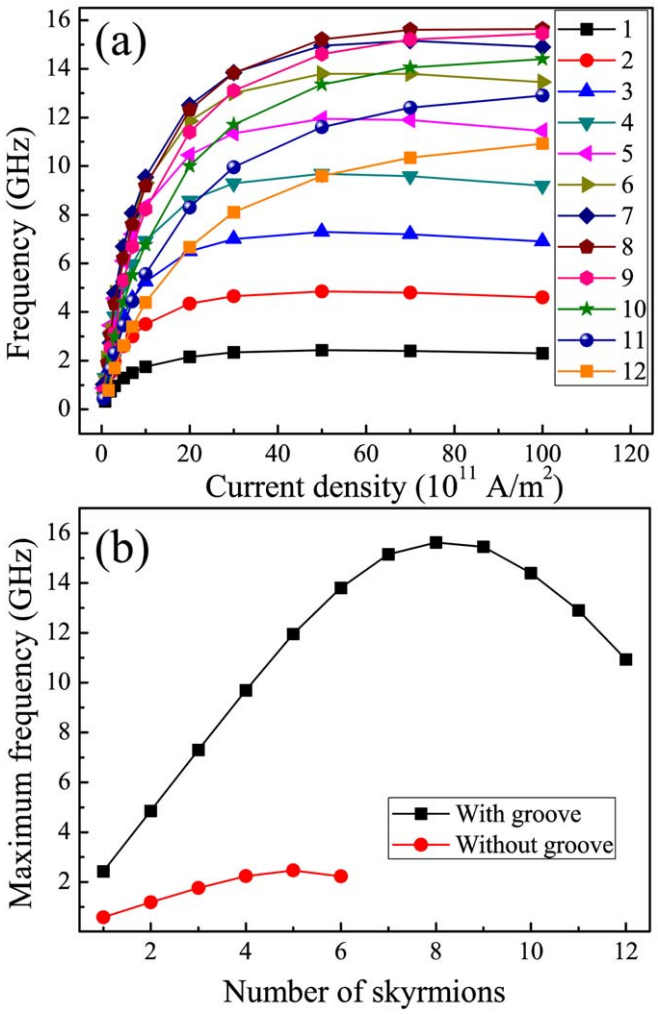

Figure 7. (a) Frequency of the STNO as a function of current density for different N. (b) Maximum Frequency as a function of N for the case with and without the presence of the annular groove.

$$\mathbf{G} \times \mathbf{v} + \mathbf{F}_{\mathrm{ST}} - \mathbf{F}_{\alpha} - \nabla U = 0, \tag{3}$$

where $\mathbf{G} = -\frac{4\pi S t_{\mathrm{F}} M_{\mathrm{s}}}{\gamma \mathbf{e}_z}$ is the gyrovector, S is the skyrmion number. For Néel skyrmions and Bloch skyrmions, $S = 1$. While for Antiskyrmios, the skyrmion number $S = -1$, which leads the gyrovector $\mathbf{G}$ of the Antiskyrmions different from that of Néel skyrmions and Bloch skyrmions. Therefore, the rotation direction of the Antiskyrmions is changed to clockwise. $\mathbf{v}$ is the velocity of the skyrmion that can be decomposed into the tangential ($\mathbf{e}_\theta$) and radial ($\mathbf{e}_\rho$) directions in polar coordinates with the form $\mathbf{v} = v_{\mathrm{t}}\mathbf{e}_\theta + v_{\mathrm{r}}\mathbf{e}_\rho$. $\mathbf{F}_{\mathrm{ST}}$ is the spin transfer force with the form $\mathbf{F}_{\mathrm{ST}} = F_{\mathrm{t}}\mathbf{e}_\theta + F_{\mathrm{r}}\mathbf{e}_\rho$, the component $F_i (i = t \text{ or } r)$ of the $\mathbf{F}_{\mathrm{ST}}$ is given by $F_i = \frac{\hbar PJ}{2e}\int \mathbf{m}_{\mathrm{p}} \cdot (\mathbf{m} \times \partial_i \mathbf{m})\mathrm{d}x\mathrm{d}y$, whose value is proportional to the current density J. $\mathbf{F}_{\alpha} = \hat{\mathbf{D}} \cdot \mathbf{v}$ is the damping force, where $\hat{\mathbf{D}}$ is the damping tensor with the value of D_α. U is the potential for the skyrmion due to the repulsive force ($\mathbf{F}_{\mathrm{ss}}$) from the nearest neighbor skyrmions and the kerb force of the annular groove ($\mathbf{F}_{\mathrm{Kerb}}$), i.e. $\nabla U = (F_{\mathrm{Kerb}} - \sum F_{\mathrm{ss}})\mathbf{e}_\rho$, where F_{ss} is inversely proportional to the distance between two skyrmions [40]. It should be noted that the potential U is also affected by the size of the nanodisk,we have demonstrated that the frequency of the STNO is inversely proportional to the radius of the nanodisk in our previous work [9]. When skyrmions moves steadily in the annular groove, which means $v_{\mathrm{r}} = 0$. Therefore, equation (3) can be written as:

$$-D_\alpha v_{\mathrm{t}}\mathbf{e}_\theta + F_{\mathrm{t}}\mathbf{e}_\theta = 0, \tag{4a}$$

$$Gv_{\mathrm{t}}\mathbf{e}_\rho - (F_{\mathrm{Kerb}} - \sum F_{\mathrm{ss}} - F_{\mathrm{r}})\mathbf{e}_\rho = 0. \tag{4b}$$

The oscillation frequency of the multiple skyrmions-based STNOs can be expressed as:

$$f = N\frac{v_{\mathrm{t}}}{2\pi r_{\mathrm{s}}}, \tag{5}$$

where r_{s} is the oscillation radius of skyrmions.

Following, we investigate the frequency dependence of current density for different N, as shown in figure 7(a). It is found that the frequency of the 12 types of STNOs shown in figure 5 all increase first and then keep unchanged with the increase in current density. Equations (4*a*) and (5) also indicate that ν_t is greatly affected by F_{ST}, that is, f increases with the increase in the current density before it reaches saturation. Figure 7(b) compares the maximum frequency dependency of N with and without the annular groove. In the presence of the annular groove, with N increases from 1 to 12, the maximum frequency of the STNO first increases from 2.43 to 15.63 GHz ($N = 8$), and then decreases to 10.93 GHz. Moreover, with α further decreases to 0.01, the skyrmions are annihilated due to the strong spin wave induced by the spin current. From equations (4*a*) and (5), it can be known that: when $N < 6$, the value of F_{ss} is almost 0 due to the long distance between two skyrmions and therefore f increases linearly with the increase in N; when $N > 6$, F_{ss} increases sharply with the decrease in the distance between two skyrmions, which leads to the decrease of ν_t. That is the reason why, although the number of skyrmions has increased, the frequency of the STNO no longer increases linearly with the increase in N or even begins to decrease. In the absence of the annular groove, the maximum frequency of the STNO also first increases and then decreases with N increases from 1 to 6, and the extreme value of the maximum frequency is 2.47 GHz when $N = 5$. It can be seen that the frequency tunability of STNOs with the annular groove is improved by 6.3 times than that of without the annular groove, and there are three reasons by analyzing equations (4*a*) and (5). First, the kerb force from the annular groove is far larger than the boundary-induced force; second, more number of skyrmions can stably locate in the annular groove because their size are restricted by the groove; third, the oscillation radius of those skyrmions are fixed in the annular groove and does not increase significantly with the increase in current density.

4. Conclusions

In summary, we proposed a skyrmion-based STNO with the presence of an annular groove. By micromagnetic simulations, we first set one skyrmion in the annular groove and demonstrate that the skyrmion can move around in the annular groove driven by a spin current. Following, we investigate the influence of the annular groove parameters including d and r on the frequency of the STNO, the results show that the oscillation frequency is inversely proportional to both d and r within a certain range under the same current density. Interestingly, the oscillation frequency with an annular is far larger than that of without an annular groove, the Thiele's equation indicates that this is because the potential of the kerb is larger than that of the boundary and the oscillation radius of the skyrmion can be controlled by the groove. Moreover, because the size of the skyrmion is restricted by the annular groove, up to 12 skyrmions can stably locate in the annular groove, which is much more than the case without the annular groove. On that basis, the frequency tunability of the STNO reaches to 15.63 GHz, which is about 6.3 times of the STNOs without the groove. Our results may provide a possibility for the design of high-frequency skyrmion-based STNOs.

Acknowledgments

This work is supported by National Science Fund of China (11574121 and 51 771 086). CJ acknowledges the funding by the China Scholarship Council.

ORCID iDs

Jianbo Wang https://orcid.org/0000-0002-4203-8336
Qingfang Liu https://orcid.org/0000-0001-6533-2880

References

[1] Zeng Z, Finocchio G and Jiang H 2013 *Nanoscale* **5** 2219–31
[2] Rippard W H, Pufall M R, Kaka S, Russek S E and Silva T J 2004 *Phys. Rev. Lett.* **92** 027201
[3] Katine J A and Fullerton E E 2008 *J. Magn. Magn. Mater.* **320** 1217–26
[4] Dussaux A *et al* 2010 *Nat. Commun.* **1** 8
[5] Grimaldi E, Dussaux A, Bortolotti P, Grollier J, Pillet G, Fukushima A, Kubota H, Yakushiji K, Yuasa S and Cros V 2014 *Phys. Rev.* B **89** 104404
[6] Ruotolo A, Cros V, Georges B, Dussaux A, Grollier J, Deranlot C, Guillemet R, Bouzehouane K, Fusil S and Fert A 2009 *Nat. Nanotechnol.* **4** 528
[7] Mohseni S M *et al* 2013 *Science* **339** 1295–8
[8] Chung S *et al* 2014 *J. Appl. Phys.* **115** 172612
[9] Zhang S, Wang J, Zheng Q, Zhu Q, Liu X, Chen S, Jin C, Liu Q, Jia C and Xue D 2015 *New J. Phys.* **17** 023061
[10] Garcia-Sanchez F, Sampaio J, Reyren N, Cros V and Kim J V 2016 *New J. Phys.* **18** 075011

[11] Jin C, Wang J, Wang W, Song C, Wang J, Xia H and Liu Q 2018 *Phys. Rev. Appl.* **9** 044007
[12] Shen L, Xia J, Zhao G, Zhang X, Ezawa M, Tretiakov O A, Liu X and Zhou Y 2019 *Appl. Phys. Lett.* **114** 042402
[13] Zhou Y, Iacocca E, Awad A A, Dumas R K, Zhang F C, Braun H B and Åkerman J 2015 *Nat. Commun.* **6** 8193
[14] Feng Y, Xia J, Qiu L, Cai X, Shen L, Morvan F J, Zhang X, Zhou Y and Zhao G 2019 *J. Magn. Magn. Mater.* **491** 165610
[15] Ono T and Nakatani Y 2008 *Appl. Phys. Express* **1** 061301
[16] Bisig A, Heyne L, Boulle O and Kläui M 2009 *Appl. Phys. Lett.* **95** 162504
[17] Martinez E, Torres L and Lopez-Diaz L 2011 *Phys. Rev.* B **83** 174444
[18] Sharma S, Muralidharan B and Tulapurkar A 2015 *Sci. Rep.* **5** 14647
[19] Nagaosa N and Tokura Y 2013 *Nat. Nanotechnol.* **8** 899
[20] Mühlbauer S, Binz B, Jonietz F, Pfleiderer C, Rosch A, Neubauer A, Georgii R and Böni P 2009 *Science* **323** 915–9
[21] Yu X Z, Onose Y, Kanazawa N, Park J H, Han J H, Matsui Y, Nagaosa N and Tokura Y 2010 *Nature* **465** 901
[22] Huang S X and Chien C L 2012 *Phys. Rev. Lett.* **108** 267201
[23] Heinze S, von Bergmann K, Menzel M, Brede J, Kubetzka A, Wiesendanger R, Bihlmayer G and Blügel S 2011 *Nat. Phys.* **7** 713
[24] Jiang W *et al* 2015 *Science* **349** 283–6
[25] Boulle O *et al* 2016 *Nat. Nanotechnol.* **11** 449
[26] Nayak A K, Kumar V, Ma T, Werner P, Pippel E, Sahoo R, Damay F, Rößler U K, Felser C and Parkin S S P 2017 *Nature* **548** 561
[27] Dzyaloshinsky I 1958 *J. Phys. Chem. Solids* **4** 241–55
[28] Moriya T 1960 *Phys. Rev.* **120** 91–8
[29] Rohart S and Thiaville A 2013 *Phys. Rev.* B **88** 184422
[30] Hoffmann M, Zimmermann B, Müller G P, Schürhoff D, Kiselev N S, Melcher C and Blügel S 2017 *Nat. Commun.* **8** 308
[31] Zhang S L, van der Laan G, Wang W W, Haghighirad A A and Hesjedal T 2018 *Phys. Rev. Lett.* **120** 227202
[32] Purnama I, Gan W L, Wong D W and Lew W S 2015 *Sci. Rep.* **5** 10620
[33] Storm A J, Chen J H, Ling X S, Zandbergen H W and Dekker C 2003 *Nat. Mater.* **2** 537–40
[34] Sampaio J, Cros V, Rohart S, Thiaville A and Fert A 2013 *Nat. Nanotechnol.* **8** 839
[35] Donahue M J and Porter D G 1999 *OOMMF User's Guide* (Gaithersburg, MD: US Department of Commerce, Technology Administration, National Institute of Standards and Technology)
[36] Brataas A, Kent A D and Ohno H 2012 *Nat. Mater.* **11** 372
[37] Jin C, Zhang C, Song C, Wang J, Xia H, Ma Y, Wang J, Wei Y, Wang J and Liu Q 2019 *Appl. Phys. Lett.* **114** 192401
[38] Papanicolaou N and Tomaras T 1991 *Nucl. Phys.* B **360** 425–62
[39] Thiele A A 1973 *Phys. Rev. Lett.* **30** 230–3
[40] Zhang X, Zhao G P, Fangohr H, Liu J P, Xia W X, Xia J and Morvan F J 2015 *Sci. Rep.* **5** 7643